Journal of Organometallic Chemistry, 382 (1990) 237–253
Elsevier Sequoia S.A., Lausanne – Printed in The Netherlands
JOM 20368

Reactivity patterns and catalytic chemistry of iridium polyhydride complexes *

Alan S. Goldman ** **and Jack Halpern** ***
Department of Chemistry, The University of Chicago, Chicago, Illinois 60637 (U.S.A.)

(Received May 18th, 1989)

Abstract

$[IrH_5P_2]$ (**1**, P = PPr^i_3) reacts autocatalytically with CF_3COOR (R = CH_2CF_3) in cyclo-C_6D_{12} at 60 °C according to: $\mathbf{1} + CF_3COOR \rightarrow [IrH_2P_2(OR)]$ (**2**) + ROH (**4**) (eq. 1). The rate-law, $-d[\mathbf{1}]/dt = k[\mathbf{1}]^{1/2}[CF_3COOR][\mathbf{2}]^{1/2}[\mathbf{4}]^{-1/2}$ ($k = 1.25 \times 10^{-4}$ $M^{-1/2}$ sec^{-1}), is consistent with the mechanism, $\mathbf{1} + \mathbf{2} \rightleftharpoons 2\ [IrH_3P_2]$ (**5**) + **4** (rapid equilibrium); $\mathbf{5} + CF_3COOR \rightarrow [IrH_2P_2\{OCH(OR)CF_3\}]$ (**6**) (rate determining); $\mathbf{6} \rightarrow \mathbf{2} + CF_3CHO$; $\mathbf{5} + CF_3CHO \rightarrow \mathbf{2}$. **2** reacts rapidly with H_2 (25 °C, 1 atm) according to: $\mathbf{2} + 2\ H_2 \rightarrow \mathbf{1} + \mathbf{4}$ (eq. 2). Although the combination of reactions 1 and 2 constitute a catalytic cycle for the hydrogenation of CF_3COOR ($CF_3COOR + 2\ H_2 \rightarrow 2$ (**4**), catalyzed by **1**), such catalytic hydrogenation does not occur, presumably because H_2 suppresses reaction by rapidly converting the catalytic intermediates, **2** and **5**, to **1**. However, **1** was found to be effective as a catalyst or catalyst precursor for transfer hydrogenation, e.g. $CH_2{=}CHC(CH_3)_3 + (CH_3)_2CHOH \rightarrow CH_3CH_2C(CH_3)_3 + (CH_3)_2C{=}O$. While not directly detected, IrH_3P_2 could be trapped at low temperatures by N_2 to yield the complexes $[IrH_3P_2(N_2)]$ and $[(IrH_3P_2)_2N_2]$ which are related through the labile equilibrium, $[(IrH_3P_2)_2N_2] + N_2 \rightleftharpoons 2\ [IrH_3P_2(N_2)]$ ($K_{eq} \sim 1.5$ at 35 °C).

Introduction

Polyhydride complexes of transition metals ($[MH_xL_y]$, where L is a ligand such as a tertiary phosphine) constitute a widespread and distinctive class of compounds whose catalytic chemistry has recently attracted considerable interest [1]. Earlier studies [2,3] have demonstrated the effectiveness of such polyhydride complexes, e.g. $[\overline{RuH_2(PPh_3)_2(PPh_2C}_6H_4)]^-$, $[RuH_4(PPh_3)_3]$, $[RuH_3(PPh_3)_3]^-$, and $[RuH_5$-

---

* Dedicated to Professor Günther Wilke on the occasion of his 65th birthday.

** Present address: Department of Chemistry, Rutgers University, New Brunswick, NJ (U.S.A.)

*** To whom correspondence should be addressed.

$(PPh_3)_2]^-$ as catalysts or catalyst precursors for the hydrogenation, not only of typical olefinic compounds, but also of a variety of other substrates such as ketones, esters and arenes that are not readily hydrogenated by most other homogeneous catalysts. In this paper we describe the extension of these studies to the iridium polyhydride complex $[IrH_5P_2]$ ($P = PPr^i_3$). A preliminary account of this work has previously appeared in communication form [4].

Results and discussion

1. Reaction of IrH_5P_2 with CF_3COOR

IrH_5P_2 (**1**, P = triisopropylphosphine) reacts with the activated ester CF_3COOR ($R = CH_2CF_3$) at 60 °C in cyclohexane-d_{12} [5*] and in tetrahydrofuran (THF)-d_8 to yield the novel complex $IrH_2P_2(OR)$ (**2**) in accord with eq. 1.

$$IrH_5P_2 + CF_3COOR \rightarrow IrH_2P_2(OR) + \underset{(4)}{ROH} \qquad (1)$$

Characterization of $IrH_2P_2(OR)$. The ^1H NMR spectrum of $IrH_2P_2(OR)$ (Table 1) exhibits a metal hydride triplet resonance (δ −31.2, $^2J(H-P)$ 13.5 Hz, 2H, IrH^a) similar to that reported for the related complexes $[P(cyclohexyl)_3]_2IrH_2Cl$ [6] and $[P(Bu^t)_3]_2IrH_2Cl$ [7]. A complex multiplet at δ 2.23 is attributable to the isopropyl protons of the *trans*-phosphine ligands (6H, $^3J(H^d-H^e)$ 7.0 Hz, $[^2J(H^d-P) + {}^4J(H^d-P)]/2 \sim 3.5$ Hz). A pseudo-quartet due to the phosphine ligand methyl groups reveals virtual coupling between the phosphorus nuclei, δ 1.23 (36 H, $[^3J(H^e-P) + {}^5J(H^e-P)]/2 \sim {}^3J(H^e-H^d) \sim 6.8$ Hz). The selectively ("aliphatic") proton-decoupled ^{31}P NMR spectrum of $IrH_2P_2(OR)$ (Table 1) exhibits a triplet, δ 51.0, with an apparent coupling constant with the hydridic protons, $^2J(H^a-P)$ 13.0 Hz.

The presence of the trifluoroethoxy group in $IrH_2P_2(OR)$ is demonstrated by a 1/3/3/1 quartet at δ 4.38 (2H, $^3J(H-F)$ 9.3 Hz) in the ^1H NMR spectrum. In the ^{19}F NMR spectrum a triplet is observed at δ −78.1 ($^3J(H^c-F)$ 9.3 Hz). The trifluoroethoxy group undergoes rapid exchange on the NMR time scale with free ROH (δ 3.76) as manifested in both the ^1H and ^{19}F NMR spectra.

Addition of CO to a solution of $IrH_2P_2(OR)$ immediately yields the colorless adduct *cis,trans*-$IrH_2P_2(OR)(CO)$ (**3**). The ^1H NMR spectrum reveals two inequivalent hydrides each split by two equivalent ^{31}P nuclei and by each other, to give two triplets of doublets. The selectively ("aliphatic") proton-decoupled ^{31}P NMR spectrum is a pseudo-triplet, δ 35.9, with an apparent coupling constant of 15 Hz (cf. H–P coupling constants of 18.4 and 13.7 Hz from ^1H NMR). The ^{19}F NMR spectrum is a triplet, δ −78.4, $^3J(H^c-F)$ 9.5 Hz, consistent with the ^1H NMR spectrum. In contrast to the coordinatively unsaturated $IrH_2P_2(OR)$ complex **2**, neither the ^1H nor ^{19}F NMR spectra reveal any evidence for exchange of the trifluoroethoxy group with free ROH. The addition of ^{13}CO to a solution of $IrH_2P_2(OR)$ yields $IrH_2P_2(OR)(^{13}CO)$, readily identified by $^{13}C-H$ coupling of its ^1H NMR hydride resonances (Table 1): δ −8.01 ($^2J(C-H)$ 41.5 Hz, $^2J(H-H)$ 5.4 Hz, IrH *trans* to CO); δ −22.0 ($^2J(C-H) \sim {}^2J(H-H) \sim 5$ Hz, IrH *cis* to CO).

The infrared spectrum of $IrH_2P_2(OR)(CO)$ contains a strong $\nu(CO)$ band at 1964.9 cm^{-1}, (cf. 1970 cm^{-1} for $IrH_2[P(cyclohexyl)_3]_2(CO)Cl$ [6]). Bands at 2092

---

* Reference number with asterisk indicates a note in the list of references.

Table 1

NMR spectral data.

Complex	IrH [a]		OCH$_2$CF$_3$	P[CH(CH$_3$)$_2$]$_3$ [a]		δ(P) [b]	^2J(H^a–P) [c]	^2J(H^b–P)	^2J(H^a–H^b)	^3J(H^c–F)	Other
	H^a	H^b	H^c	H^d	H^e						
IrP$_2$H$_5$ (**1**)	–11.26 (t)	–	–	1.76 (m)	1.11 (q [d])	44.7	12.4	–	–	–	
IrP$_2$H$_2$(OR) (**2**)	–31.2 (t)	–	4.38 (t)	2.23(m)	1.23 (q [d])	51.0	13.5	–	–	9.3	^{19}F NMR: δ –78.1 [e]
IrP$_2$H$_2$(CO)(OR) (**3**)	–21.9 (td)	–7.99 (td)	3.93 (q)	2.35 (m)	1.25 (m)	35.9	13.7	18.4	5.3$_3$	9.5	^{19}F NMR: δ –78.4 [e]
IrP$_2$H$_2$(^{13}CO)(OR)	–22.0 (tt)	–8.01 (dtd)	3.93 (q)	2.35 (m)	1.25 (m)	–	13.8	18.4	5.3$_6$	9.8	^2J(H^a–^{13}C) ~ 4.8; ^2J(H^b–^{13}C) = 41.5
IrP$_2$H$_3$(N$_2$) (**8**)	–11.1 (td)	–19.7 (tt)	–	1.89 (m)	1.19 (m)	44.8	15.5	17	~ 4.5	–	^2J(H^b–^{15}N^a) 21; ^3J(H^b–^{15}N^b) ~ 4.5 ^2J(H^a–^{15}N) < 1.5 [f]; ^2J(P–^{15}N^a) 2.1
(IrP$_2$H$_3$)$_2$(N$_2$) (**9**)	–11.2 (td)	–21.6 (tt)	–	1.94 (m)	1.29 (m)	47.7	16	18	4.$_3$	–	
(IrP$_2$H$_3$)$_2$(^{15}N$_2$)	–11.2 (td)	–21.6 (m)	–	1.95 (m)	1.29 (m)	47.7	16	18	~ 4	–	^2J(H^b–^{15}N^a) 21.3; ^3J(H^b–^{15}N^b) ~ 4 [f] ^3J(P–^{15}N^a) 1.8

[a] See structures in text for assignments. [b] Relative to H$_3$PO$_4$. [c] ^2J(H–P) coupling values taken from ^{1}H NMR; values from selectively decoupled ^{31}P NMR slightly less due to partial decoupling. [d] Pseudo-quartet: [^3J(H–P) + ^3J(H–P)]/2 ~ ^3J(H–H) ~ 7 Hz; in other cases a more complex pattern is observed. [e] Relative to CCl$_3$F. [f] J(H–N) values obtained from complex multiplets with use of NICSIM simulation program.

and 2165 cm^{-1} may be attributable to Ir–H stretching frequencies (cf. 2100, 2200 cm^{-1} for $IrH_2[P(cyclohexyl)_3]_2(CO)Cl$ [6]).

Molecular weight determinations of $IrH_2P_2(OR)$ yielded values of $(1.03 \pm 0.10) \times$ (calculated MW of monomer). ^1H NMR measurements revealed no concentration dependence of the spectrum over a range of 1.2–64 mM; thus $IrH_2P_2(OR)$ appears to be monomeric with no significant equilibrium dimer concentration in this range. In spite of this apparent coordinative unsaturation, no evidence for reaction (24 h, 25 °C) was observed by ^1H NMR upon addition of free PPr^i_3 (5.0×10^{-2} M) to a solution of $IrH_2P_2(OR)$ (6.4×10^{-2} M). All these observations are consistent with structure **2a** or **2b** for $IrH_2P_2(OR)$ and with structure **3** for $IrH_2P_2(OR)(CO)$.

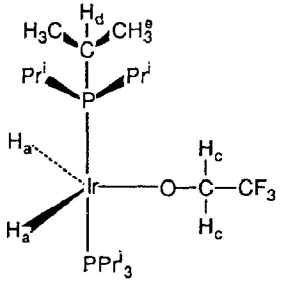

2a

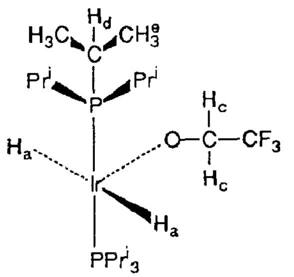

2b

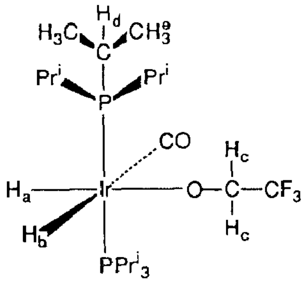

3

$IrH_2P_2(OR)$ was synthesized independently by the reaction of IrH_5P_2 with 3,3-dimethylbutene (eq. 2).

$$IrH_5P_2 + 2\ CH_2{=}CHC(CH_3)_3 + ROH \xrightarrow[\text{cyclohexane}]{24\ \text{h},\ 25\,^\circ C} IrH_2P_2(OR) + 2\ CH_3CH_2C(CH_3)_3 \quad (2)$$

(3,3-Dimethylbutane was identified by ^1H NMR when the reaction was conducted in C_6D_{12}). This independent synthesis provides support for the proposed formulation and serves as a convenient synthetic method which was used to prepare the $IrH_2P_2(OR)$ used in the experiments described in this paper.

Finally, in support of the proposed formulation it was found that $IrH_2P_2(OR)$ reacts immediately with H_2 at room temperature to yield IrH_5P_2 and ROH (eq. 3):

$$IrH_2P_2(OR) + 2\ H_2 \xrightarrow{\text{fast}} IrH_5P_2 + ROH \quad (3)$$

Kinetics of reaction 1. Although the combination of eq. 1 and 3 constitutes a catalytic cycle for the hydrogenation of CF_3COOR, reaction 1 does not proceed under an H_2 atmosphere. Thus, a solution of IrH_5P_2 (1.5×10^{-2} M) and CF_3COOR (0.16 M) under one atm H_2 showed no sign of reaction after 80 h at 80 °C.

In the absence of H_2, reaction 1 was preceded by an induction period of ca. 1 h, under the conditions typically employed (1.5×10^{-2} M IrH_5P_2, 0.6 M CF_3COOR, 60 °C). However, initial addition of $IrH_2P_2(OR)$ eliminated the induction period. Kinetic measurements encompassing the initial concentration ranges 3.3×10^{-3} to 1.2×10^{-2} M IrH_5P_2, 2.4×10^{-2} to 1.4×10^{-1} M $IrH_2P_2(OR)$, 6.0×10^{-2} to 4.0×10^{-1} M CF_3COOR, and 2.6×10^{-3} to 4.1×10^{-2} M ROH, yielded the rate law eq. 4, with $k_2 = 1.25 \times 10^{-4}$ $M^{-1/2}s^{-1}$ at 60 °C.

$$-d[IrH_5P_2]/dt = k_2[IrH_5P_2]^{1/2}[IrH_2P_2(OR)]^{1/2}[CF_3COOR][ROH]^{-1/2} \quad (4)$$

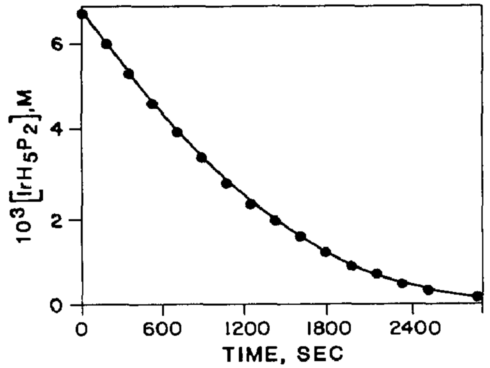

Fig. 1. Pseudo-half-order rate plot for reaction 1 at 60 °C. Initial concentrations: 6.9×10^{-3} *M* IrH_5P_2, 0.40 *M* CF_3COOR, 0.039 *M* $IrH_2P_2(OR)$, 0.65 *M* ROH.

Under pseudo-half-order conditions ($IrH_2P_2(OR)$, CF_3COOR, and ROH in excess), the rate law reduces to eq. 5.

$$-d[IrH_5P_2]/dt = k_{obsd}[IrH_5P_2]^{1/2} \tag{5}$$

$$k_{obsd} = k_2[IrH_2P_2(OR)]^{1/2}[CF_3COOR][ROH]^{-1/2} \tag{6}$$

In accord with this, reaction 1 was found to exhibit pseudo-half-order kinetics (Fig. 1) with values of k_{obsd} which were found to be independent of the initial IrH_5P_2 concentration (3.3×10^{-3} to 1.2×10^{-2} *M*) and to exhibit the dependencies on $[IrH_2P_2(OR)]$, $[CF_3COOR]$, and [ROH] described by eq. 6 (Fig. 2–4).

This kinetic behavior can be accomodated by the following mechanistic scheme, according to which $k_2 = (K_5^{eq})^{1/2}k_6$.

$$IrH_5P_2 + IrH_2P_2(OR) \underset{\text{rapid equilibrium}}{\overset{K_5^{eq}}{\rightleftharpoons}} \underset{(5)}{2\,IrH_3P_2} + ROH \tag{7}$$

$$IrH_3P_2 + CF_3COOR \xrightarrow[\text{rate determining}]{k_6} \underset{(6)}{IrH_2P_2[OCH(OR)CF_3]} \xrightarrow{\text{fast}} IrH_2P_2(OR) + CF_3CHO \tag{8}$$

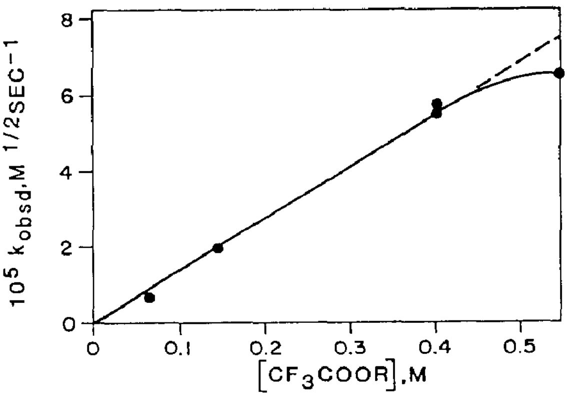

Fig. 2. Dependence of k_{obsd} on $[CF_3COOR]$. Initial concentrations: 3.2×10^{-2} *M* $IrH_2P_2(OR)$; 1.2×10^{-2} *M* IrH_5P_2; 6.5×10^{-2} *M* ROH.

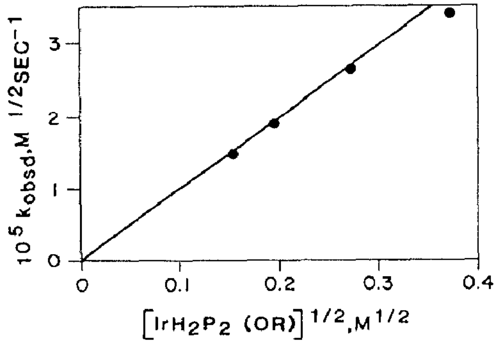

Fig. 3. Dependence of k_{obsd} on $[IrH_2P_2(OR)]$. Initial concentrations: 0.136 *M* CF_3COOR; 6.5×10^{-2} *M* ROH.

$$IrH_3P_2 + CF_3CHO \xrightarrow{\text{fast}} IrH_2P_2(OR) \qquad (9)$$

Support for the proposed role of $IrH_2P_2(OR)$ as an "H_2 sponge" (eq. 7) is provided by our finding that addition of ca. 5×10^{-3} *M* of another efficient H_2 acceptor, $IrI(CO)(PPh_3)_2$, in place of $IrH_2P_2(OR)$ also resulted in elimination of the induction period of reaction 1, presumably by generating IrH_3P_2 through reaction 10.

$$IrH_5P_2 + IrI(CO)(PPh_3)_2 \rightarrow IrH_3P_2 + IrH_2I(CO)(PPh_3)_2 \qquad (10)$$

At high concentration of CF_3COOR and $IrH_2P_2(OR)$ (Fig. 2 and 3) the rate of reaction 1 tended to depart from the rate law of eq. 6 and to level off. This is attributable to reaction 7 becoming rate-limited by the reductive elimination of H_2, k_{10}, according to the scheme of eq. 11 and 12. Equilibria 7 and 11 both lie far to the left, thus precluding direct observation of IrH_3P_2.

$$IrH_5P_2 \underset{k_{-10}}{\overset{k_{10}}{\rightleftharpoons}} IrH_3P_2 + H_2 \qquad (11)$$

$$H_2 + IrH_2P_2(OR) \rightarrow IrH_3P_2 + ROH \qquad (12)$$

Above 0.04 *M* ROH the rate of reaction 1 was found to increase with increasing ROH concentration. This is attributable to a medium effect. Consistent with this, it

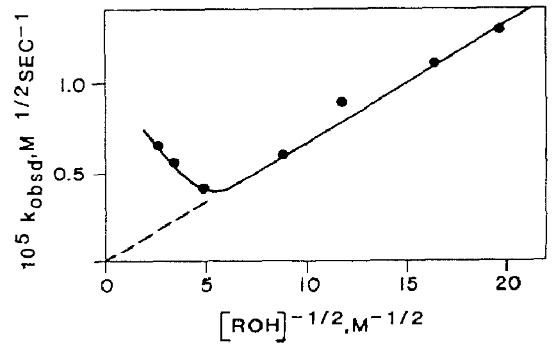

Fig. 4. Dependence of k_{obsd} on [ROH]. Initial concentrations: 5×10^{-3} *M* IrH_5P_2; 0.04 *M* CF_3COOR; 1.84×10^{-2} *M* $IrH_2P_2(OR)$. For experiments at low initial ROH concentrations, k_{obsd} was deduced from initial rate measurements so that $IrH_2P_2(OR)$ and ROH concentrations were effectively constant.

was found that addition of an inert polar solvent, 2,2,5,5-tetramethyltetrahydrofuran also increased the reaction rate.

Rate of H_2 reductive elimination as determined by substitution reactions. The rate constant of the H_2 loss step (k_{10}) for reaction 5 was determined independently by measurements of the kinetics of the reaction of IrH_5P_2 with several two-electron donor ligands, L, eq. 13.

$$IrH_5P_2 \underset{H_2\,(k_{-10})}{\overset{H_2\,(k_{10})}{\rightleftharpoons}} IrH_3P_2 \xrightarrow{L\,(k_{11})} IrH_3P_2L \qquad (13)$$

In all cases the reaction proceeded to completion. The *mer* configuration of the IrH_3P_2L products were assigned by comparison of their ^1H NMR spectra with those of known $IrH_3(PEtPh_2)_2L$ analogues [8].

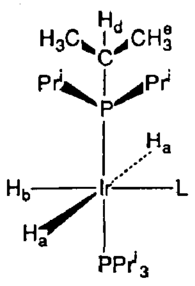

7

No evidence for dissociation of PPr^i_3 from IrH_5P_2, i.e., no free PPr^i_3 or products containing less than two PPr^i_3 ligands, was detected.

$P(OMe)_3$ (0.038 to 0.52 *M*) was treated with IrH_5P_2 (5.7×10^{-3} to 2.4×10^{-2} *M*) according to eq. 13. Due to the slow equilibration of H_2 between gas and solution phases, the concentration of H_2 in solution (3.0×10^{-3} to 1.4×10^{-2} *M*, monitored by ^1H NMR) remained approximately constant (±10%) in each experiment after ca. 75% completion. Monitoring of the kinetics in this region yielded a linear plot of $[k_{obsd}]^{-1}$ vs. $[H_2]/[P(OMe)_3]$ in accord with the rate law (eq. 14) deduced for the dissociative substitution mechanism of eq. 13 (Fig. 5). The values of k_{10} at 60 °C, determined from the intercept of this plot, is $(4.9 \pm 0.5) \times 10^{-3}$ s^{-1}. Corresponding measurements on the reaction of cyclo-$C_6H_{11}NC$ (0.06 *M* to 0.4 *M*) with IrH_5P_2 (0.01 *M*) yielded $k_{10} = (5.7 \pm 0.6) \times 10^{-3}$ s^{-1}, in agreement with the above values (Fig. 5).

$$1/k_{obsd} = 1/k_{10} + k_{-10}[H_2]/k_{10}k_{11}[L] \qquad (14)$$

Similar results were obtained in corresponding, although less extensive, studies on reaction 13 for $L = PMe_2Ph$ and PPh_3. These yielded the following values of k_{11}/k_{-10} at 60 °C: H_2 (1.0); cyclo-$C_6H_{11}NC$ (0.68); $P(OMe)_3$ (0.096); PMe_2Ph (0.075); PPh_3 (0.02). Qualitative confirmation of the loss of H_2 from IrH_5P_2 (eq. 11) was provided by observation of exchange with D_2 under the same conditions as the various substitution reactions.

To determine whether reaction 1 proceeds through initial reductive elimination of H_2, the kinetics were measured under limiting conditions, i.e., low initial $[IrH_5P_2]$ (4.3×10^{-3} *M*), high $[CF_3COOR]$ (1.05 *M*), and high $[IrH_2P_2(OR)]$ (1.45×10^{-1} *M*), in the absence of added ROH. Although the high concentrations of CF_3COOR and $IrH_2P_2(OR)$ (i.e., large background NMR signals) and the fast time scale

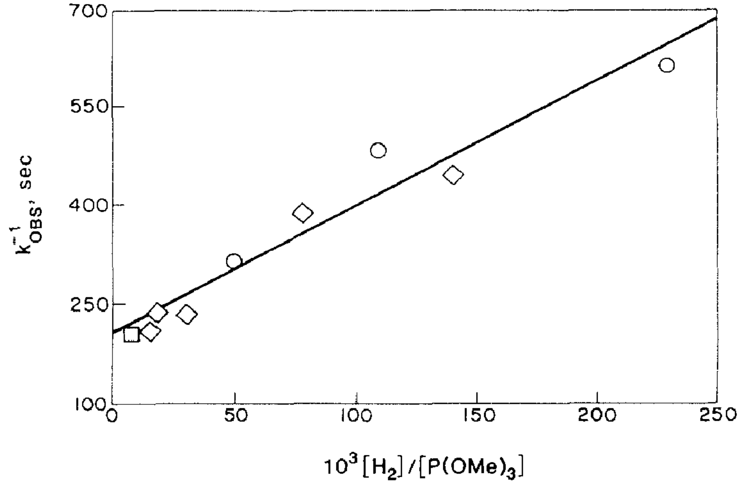

Fig. 5. Dependence of k_{obsd} on $[H_2]/[P(OMe)_3]$ at 60 °C according to eq. 14. Initial concentrations: □, 11.6×10^{-3} *M* IrH_5P_2, 3.0×10^{-3} *M* $[H_2]$, 3.8×10^{-2} *M* $P(OMe)_3$. ◇, 12×10^{-3} *M* IrH_5P_2, 9×10^{-3} *M* $[H_2]$, 6.2×10^{-2} to 5.2×10^{-1} *M* $P(OMe)_3$. ○, 5.7×10^{-3} to 24.4×10^{-3} *M* IrH_2P_5, 4.5×10^{-3} to 14×10^{-3} *M* H_2, 8.0×10^{-3} *M* $P(OMe)_3$.

introduced considerable error into the kinetic measurements, a least squares first order fit of the data yielded $k_{obsd} = (5.3 \pm 1.0) \times 10^{-3}$ s^{-1}, in good agreement with the rate constant for H_2 reductive elimination (k_{10}) determined from kinetic measurements on reaction 13. This supports the mechanism of eq. 11 and 12 for reaction 7 and explains the levelling off of k_{obsd} at high CF_3COOR concentration in Fig. 2.

II. Observation of $(P_2IrH_3)_n(N_2)$ ($n = 1, 2$)

The equilibrium of eq. 7 lies far to the left so that no IrH_3P can be detected in solutions containing IrH_5P_2 and $IrH_2P_2(OR)$. Addition of H_2 to an excess of $IrH_2P_2(OR)$ results in only partial conversion to IrH_5P_2 and ROH, eq. 3. In an attempt to observe possible intermediates in reaction 12 (such as $IrH_4P_2(OR)$ or $IrH_3P_2(HOR)$ we treated $IrH_2P_2(OR)$ with H_2 at low temperatures. Although no such intermediates were observed directly, it proved possible to trap "IrH_3P_2" as labile N_2 adducts. Thus, addition of a 90/10 N_2/H_2 gas mixture to a toluene-d_8 solution of $IrH_2P_2(OR)$ at −40 °C, yielded (together with ROH) a mixture of two species, $(IrH_3P_2)_n(N_2)$, $n = 1$ and 2, presumably through the reaction sequence of eq. 15–17.

$$IrH_2P_2(OR) + H_2 \rightarrow [IrH_3P_2] + ROH \tag{15}$$

$$[IrH_3P_2] + N_2 \rightarrow \underset{\mathbf{(8)}}{IrH_3P_2(N_2)} \tag{16}$$

$$IrH_3P_2(N_2) + [IrH_3P_2] \rightarrow \underset{\mathbf{(9)}}{(IrH_3P_2)_2(N_2)} \tag{17}$$

The ^1H NMR spectra of **8** and **9** were in good agreement with those of known *mer*-$IrH_3(PR_3)_2L$ complexes [8], including the *mer*-IrH_3P_2L complexes identified in this study (L = PPh_3, PMe_2Ph, $P(OMe)_3$, $C_6H_{11}NC$). The $^{31}P\{^1H\}$ NMR and selectively ("aliphatic") proton-decoupled ^{31}P NMR spectrum confirmed the presence of the characteristic A_2X_2X' spin system. The ^{31}P and ^1H NMR spectra of the $^{15}N_2$ analogues revealed ^{15}N–P coupling (2 Hz) for both complexes, as well as coupling between the *trans* proton and both the near and distant N nuclei (Table 1). These data are consistent with the structures **8** and **9**. Shifting the equilibrium of eq. 18 by the addition and removal of N_2 (two cycles) enabled the determination of the respective assignments of the two species and yielded a value of ca. 1.5 for K_{18} (see Experimental Section). Treatment of the solution with CO and subsequent warming to room temperature resulted in formation of *mer*-$IrH_3P_2(CO)$ (^1H NMR) (eq. 19).

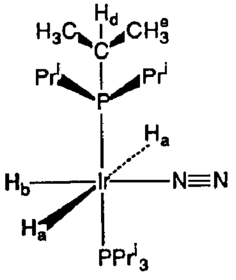

8

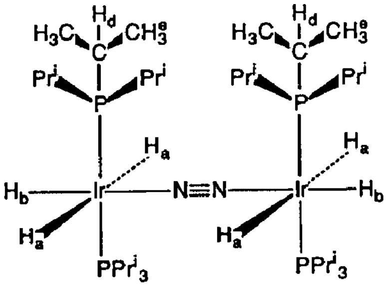

9

$$(IrH_3P_2)_2(N_2) + N_2 \overset{K_{18}^{eq}}{\rightleftharpoons} 2\ IrH_3P_2(N_2) \qquad (18)$$

$$(IrH_3P_2)_n(N_2) + n\ CO \rightarrow n\ IrH_3P_2(CO) + N_2 \qquad (19)$$

A noteworthy observation relates to the fate of the dinitrogen complexes upon warming in the presence of ROH. (No attempts were made to separate the complexes from the ROH which is a co-product of their formation reaction, eq. 15–17). After a solution containing IrH_5P_2 (1.4×10^{-3} *M*), $IrH_2P_2(OR)$ (0.4×10^{-3} *M*), $IrH_3P_2(N_2)$ (1.9×10^{-3} *M*), and $(IrH_3P_2)_2(N_2)$ (1.2×10^{-3} *M*), was warmed to room temperature for ca. 20 s, it was found to contain IrH_5P_2 (3.8×10^{-3} *M*) and $IrH_2P_2(OR)$ (2.5×10^{-3} *M*). Thus, $IrH_3P_2(N_2)_n$ ($n = 1$ or $1/2$) (4.3×10^{-3} *M*) was converted to IrH_5P_2 (2.4×10^{-3} *M*) and $IrH_2P_2(OR)$ (2.1×10^{-3} *M*), conforming, within experimental error to the stoichiometry of eq. 20.

$$2\ IrH_3P_2(N_2)_n\ (n = 1 \text{ or } 1/2) + ROH \rightarrow IrH_5P_2 + IrH_2P_2(OR) + 2n\ N_2 \qquad (20)$$

Omitting the dinitrogen, eq. 20 reduces to eq. 21, i.e., the reverse of reaction 7, the initial equilibrium step of the proposed mechanism of the reaction of IrH_5P_2 with CF_3COOR (eq. 1).

$$2\ IrH_3P_2 + ROH \rightleftharpoons IrH_5P_2 + IrH_2P_2(OR) \qquad (21)$$

III. Reactions of IrH_5P_2 with cyclohexanone and cyclohexanol

In contrast to our findings with CF_3COOR, the hydrogenation of cyclohexanone by IrH_5P_2 appeared to be promoted by an H_2 atmosphere. In a solution containing initially 1.5×10^{-2} *M* IrH_5P_2 and 0.08 *M* cyclohexanone under H_2, hydrogenation of the cyclohexanone to cyclohexanol (eq. 22) proceeded to the extent of 80% with no loss of IrH_5P_2 after 19 h at 80 °C.

$$C_6H_{10}{=}O + H_2 \xrightarrow{IrH_5P_2} C_6H_{11}OH \qquad (22)$$

In the absence of H_2 only ca. 10% of cyclohexanone reacted after 22 h at 85 °C to give unidentified products. After 4 days > 50% of IrH_5P_2 had decomposed to a complex mixture of products.

The apparent lack of reactivity of IrH_5P_2 towards cyclohexanone in the absence of H_2 can be attributed to thermodynamic, rather than kinetic, factors. When cyclohexanol (3×10^{-2} M) was added to a solution of $IrH_2P_2(OR)$ (1.5×10^{-2} M), the formation of IrH_5P_2 (7.4×10^{-3} M) was observed within ca. 15 min. After 2 h at 35 °C the concentration of IrH_5P_2 was 10.5×10^{-3} M; subsequent heating afforded no further change indicating the attainment of the equilibrium 23.

$$2\ C_6H_{11}OH + IrH_2P_2(OR) \rightleftharpoons 2\ C_6H_{10}{=}O + IrH_5P_2 + ROH \qquad (23)$$

$$K_{23} = [ROH][IrH_5P_2][C_6H_{10}{=}O]^2/[IrH_2P_2(OR)][C_6H_{11}OH]^2 \qquad (24)$$

The equilibrium constant, K_{23}, was found to be 2.4×10^{-2} M. Immediately after addition of ROH (0.114 M) to this solution the concentration of IrH_5P_2 was found to be 9.8×10^{-3} M; after 2 h at 35 °C the concentration of IrH_5P_2 had stabilized at 6.3×10^{-3} M, in accord with the equilibrium of eq. 23. Thus it appears that in the absence of H_2 hydrogenation of cyclohexanone by IrH_5P_2 (back-reaction of eq. 23) does occur but apparently ROH is required to trap the resulting dehydrogenated iridium species.

Kinetic measurements reveal that the back-reaction of eq. 23, i.e. the reaction of IrH_5P_2 (10×10^{-3} M) with cyclohexanone (and ROH), at 40 °C occurs at a rate of $(5.7 \pm 0.9) \times 10^{-4}$ s^{-1} $[IrH_5P_2]$, independent of $[C_6H_{10}O]$ (0.06 M to 0.8 M), [ROH] (0.03 M to 0.14 M) and $[IrH_2P_2(OR)]$ (0.0 to 7.5×10^{-3} M) in agreement with the rate of reductive elimination of H_2 (k_{10}) at 40 °C determined to be 5.3×10^{-4} s^{-1} from measurements of the rate of replacement of H_2 by Bu^nNC. Thus the hydrogenation of cyclohexanone by IrH_5P_2, like that of CF_3COOR, appears to proceed by a mechanism involving initial reductive elimination of H_2.

IV. Transfer hydrogenation

In light of the mechanism of eq. 7–9, 11 and 12, it is clear why H_2 suppresses the reaction of IrH_5P_2 with CF_3COOR; H_2 reacts rapidly with the reactive intermediate IrH_3P_2 (as well as with $IrH_2P_2(OR)$ to regenerate IrH_5P_2). While this behavior would appear to limit the utility of IrH_5P_2 as a hydrogenation catalyst using H_2, the chemistry that we have identified should be conducive to pathways for transfer hydrogenation [9*,10]. The observation of reaction 23 suggests that alcohols should serve as effective sources of hydrogen for catalytic transfer hydrogenation reactions. Isopropanol was preferred over cyclohexanol as a hydrogen-donor because of its simpler ^1H NMR spectrum, and because the dehydrogenation of isopropanol is thermodynamically more favorable than that of cyclohexanol ($\Delta H°$ 13.2 kcal/mol vs. 15.4 kcal/mol [11]). Consistent with this, reaction 25 was found to reach equilibrium at room temperature within ca. 5 min after mixing, with an equilibrium constant of 3.6 M.

$$IrH_2P_2(OR) + 2(CH_3)_2CHOH \rightleftharpoons IrH_5P_2 + 2(CH_3)_2C{=}O + ROH \qquad (25)$$

Reaction of IrH_5P_2 with 3,3-dimethylbutene in the absence of alcohol. 3,3-Dimethylbutene ($CH_2{=}CHCMe_3$) was selected as a prototypical olefin for the purposes of studying the transfer-hydrogenation of olefins by alcohols. In the absence of

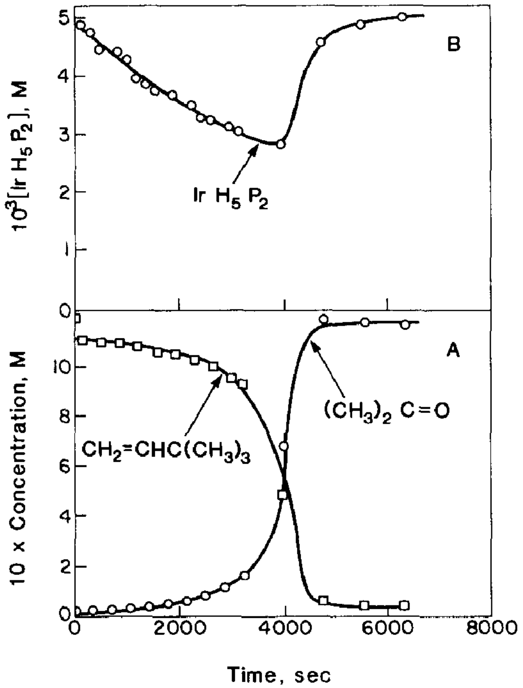

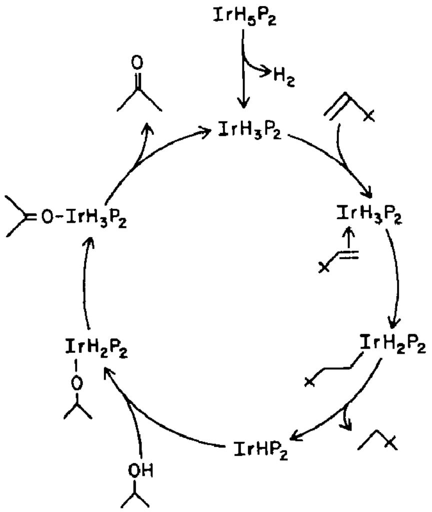

Fig. 6. IrH_5P_2-catalyzed transfer hydrogenation of CH_2=CHC$(CH_3)_3$ by $(CH_3)_2$CHOH at 30° C. Initial concentrations: 5×10^{-3} *M* IrH_5P_2, 0.6 *M* $(CH_3)_2$CHOH.

Fig. 7. Proposed mechanism of the transfer hydrogenation of the IrH_5P_2-catalyzed transfer hydrogenation of CH_2=CHC$(CH_3)_3$ by $(CH_3)_2$CHOH.

alcohols the reaction of IrH_5P_2 (1.5×10^{-2} *M*) and CH_2=$CHCMe_3$ (5.0×10^{-2} *M*) resulted in complete hydrogenation of CH_2=$CHCMe_3$ to $CH_3CH_2CMe_3$ after 4 h [12*]. This was accompanied by decomposition of IrH_5P_2 and formation of a red Ir-containing compound which did not exhibit a ^{1}H NMR signal. It was unreactive towards H_2.

Measurements of the kinetics of the reaction of IrH_5P_2 with CH_2=$CHCMe_3$ yielded the rate law $-d[IrH_5P_2]/dt = k_{obsd}[IrH_5P_2]$ where $k_{obsd} = (5.1 \pm 0.1)\times10^{-4}$ s^{-1} at 40° C, independent of [CH_2=$CHCMe_3$] (0.1, 0.5 *M*). Agreement of this value with that determined previously for k_{10} suggests that the rate-determining step is the same as that of reaction 10, i.e., reductive elimination of H_2. The corresponding rate of IrH_5P_2 (1.5×10^{-2} *M*) catalyzed hydrogenation of CH_2=$CHCMe_3$ (0.1 *M*) under an atmosphere of H_2 was much lower (ca. 1.0×10^{-3} *M* $CH_3CH_2CMe_3$/h). Under these conditions no decomposition of IrH_5P_2 occurred.

Transfer-hydrogenations of CH_2=$CHCMe_3$ by i-PrOH. In the presence of IrH_5P_2 (5×10^{-3} *M*), the reaction between i-PrOH (0.6 *M*) and CH_2=$CHCMe_3$ (0.12 *M*) (eq. 26) proceeded slowly at 30° C for ca. 1 h and then went rapidly to completion in the following 30 min (Fig. 6).

$$(CH_3)_2CHOH + CH_2{=}CHCMe_3 \xrightarrow{IrH_5P_2} (CH_3)_2CO + CH_3CH_2CMe_3 \qquad (26)$$

The reaction was monitored by ^{1}H NMR. During the initial "slow" induction phase of the reaction the concentration of IrH_5P_2 decreased by ca. 50% in an approximately first order manner ($-d\ln[IrH_5P_2]/dt = 1.6 \times 10^{-4}$ s^{-1}) and then returned to its initial value after all the CH_2=$CHCMe_3$ was consumed. The observation that the IrH_5P_2 concentration passes through a minimum when the rate of reaction between i-PrOH and CH_2=$CHCMe_3$ is a maximum suggests that IrH_5P_2 is converted reversibly to the active catalyst during the induction period. Unfortunately, attempts to characterize this transient species failed and the only species that could be detected by NMR during the course of the reaction was IrH_5P_2.

The kinetics of this system proved complex and have, thus far, eluded quantitative characterization. However, the following features have been identified.

1. The reaction is promoted by acetone, one of the products, and this presumably accounts for the initial autocatalytic phase. When 0.19 *M* acetone was added to a solution containing 5×10^{-3} *M* IrH_5P_2, 0.12 *M* CH_2=$CHCMe_3$, and 0.6 *M* i-PrOH, reaction 26 proceeded very rapidly at 30 °C, without any induction period, hydrogenation of CH_2=$CHCMe_3$ being complete in 5 min. A possible explanation for this is that the transient catalytic species is the analog of that of reaction 1, i.e. $IrH_2P_2(OCHMe_2)$, formed by reaction 27.

$$IrH_5P_2 + 2(CH_3)_2C{=}O \rightleftharpoons IrH_2P_2[OCH(CH_3)_2] + (CH_3)_2CHOH \qquad (27)$$

2. The rate of reaction 26 is highly temperature-dependent. At 20 °C the time for complete reaction for comparable initial concentration conditions (5×10^{-3} *M* IrH_5P_2, 0.12 *M* CH_2=$CHCMe_3$, 0.6 *M* i-PrOH, 0.19 *M* acetone) was ca. 80 min vs. 5 min at 30 °C. This 16-fold rate difference may reflect the cumulative contributions from increased rates of both catalyst formation and turnover.

3. The rate of reaction is inversely dependent on the CH_2=$CHCMe_3$ concentration. Thus, the time for completion of reaction 26 at 20 °C in a solution containing 5×10^{-3} *M* IrH_5P_2, 4×10^{-2} *M* CH_2=$CHCMe_3$, 0.6 *M* i-PrOH, and 0.19 *M* acetone, was ca. 20 min. When the initial CH_2=$CHCMe_3$ concentration was 0.3 *M* only 7.4×10^{-3} *M* CH_2=$CHCMe_3$ was hydrogenated after 24 min (> 7-fold rate reduction). The transfer-hydrogenation of other olefins, including 1,1-diphenylethylene and α-methylstyrene (eq. 28) exhibited similar behavior.

$$(CH_3)_2CHOH + CH_2{=}CRPh \xrightarrow{IrH_5P_2} (CH_3)_2C{=}O + CH_3CHRPh \ (R = Ph, Me) \qquad (28)$$

4. IrH_5P_2 is not the active catalyst. This conclusion was already reached in earlier studies on the reaction of IrH_5P_2 with CH_2=$CHCMe_3$ and with CF_3COOR. It is further supported by our observations that (i) reaction 26 accelerates as the concentration of IrH_5P_2 in solution is observed to decrease (Fig. 6), (ii) the transfer-hydrogenation reactions 26 and 28, as well as the reaction of CF_3COOR with IrH_5P_2, are completely inhibited by H_2. It is noteworthy that in reaction 26, IrH_5P_2 is regenerated after the olefin is consumed and that subsequent addition of more olefin results in the same reaction kinetics as obtained for the original solution. Thus it appears that after completion of the reaction the active catalyst is converted (presumably by reaction with i-PrOH) back to IrH_5P.

V. Reactions with aldehydes and primary alcohols.

Our studies with both secondary alcohols and with esters (which yield primary alcohols when hydrogenated, cf. eq. 1) prompted us to examine the reactions of

$IrH_2P_2(OR)$ with two primary alcohols, methanol and ethanol. In neither case did we obtain the simple dehydrogenated product, i.e., formaldehyde or acetaldehyde.

Reaction of $IrH_2P_2(OR)$ with methanol. Addition of MeOH (1.5×10^{-2} *M*) to a solution of $IrH_2P_2(OR)$ ($R = CH_2CF_3$; also 1.5×10^{-2} *M*) resulted in the formation of IrH_5P_2 and $IrH_3P_2(CO)$ in qualitative accord with eq. 29.

$$3\ IrH_2P_2(OR) + 2\ CH_3OH \rightarrow 2\ IrH_3P_2(CO) + IrH_5P_2 + 3\ ROH \qquad (29)$$

After ca. 10 min. at 31° C the solution contained 6.1×10^{-3} *M* $IrH_2P_2(OR)$, 6.8×10^{-3} *M* MeOH, 2.7×10^{-3} *M* IrH_5P_2 and 4.3×10^{-3} *M* $IrH_3P_2(CO)$. Further standing (ca. 12 h) resulted in little further reaction.

It is noteworthy that there was no indication of the formation of $IrH_2P_2(OMe)$, i.e., neither the IrH nor CF_3CH_2O resonances of $IrH_2P_2(OR)$ were shifted by the presence of MeOH. In view of the rapid exchange of the OCH_2CF_3 group of $IrH_2P_2(OR)$ with ROH, this is presumably due to thermodynamic rather than kinetic factors.

Reaction of $IrH_2P_2(OR)$ with EtOH. Addition of EtOH (0.04 *M*) to a solution of $IrH_2P_2(OR)$ (ca. 25×10^{-3} *M*) led to a color change from orange to pale orange-yellow over ca. 2 min. The ^1H NMR spectrum of the resulting solution revealed the formation of IrH_5P_2 (14×10^{-3} *M*), $IrH_3P_2(CO)$ (2.1×10^{-3} *M*), and *cis,trans*-$IrH_2P_2(CH_3)(CO)$ (11×10^{-3} *M*). The latter was identified by its ^1H NMR spectrum containing two inequivalent hydride resonances and a signal attributable to a metal-coordinated methyl group: δ −11.84 (1H, t of d, $^2J(HP)$ 15.2, $^2J(HH) \sim 5.2$ Hz, IrH (*cis* to CO?)), δ −13.34 (1H, t of d, $^2J(HP)$ 16.5, $^2J(HH) \sim 5.5$ Hz, IrH (*trans* to CO?)), δ −0.35 (2.7H, broad, "incompletely resolved triplet", $IrCH_3$), δ 2.22 (6.8H, m, $P(CHMe_2)_3$). The organic products were ROH (δ 3.75, q, $J(HF)$ 8.6 Hz) and, surprisingly, ethyl acetate, $MeCO_2Et$ (7×10^{-3} *M*) (^1H NMR: δ 4.013, 2H, q, $^3J(HH)$ 7.2 Hz, $CH_3CO_2CH_2CH_3$ and δ 1.876, 3H, s, $CH_3CO_2CH_2CH_3$). This was in agreement with an authentic sample of pure $MeCO_2Et$ in C_6D_{12} (the $CH_3CO_2CH_2CH_3$ signal (δ 1.175) overlapped with the phosphine ligand methyl peaks and was not identified in the reaction mixture). When authentic $MeCO_2Et$ was added to the product mixture, peak enhancements were observed for both signals. These observations are consistent with reactions 30 and 31.

$$IrH_2P_2(OR) + 2\ EtOH \rightarrow IrH_5P_2 + ROH + CH_3COOEt \qquad (30)$$

$$3\ IrH_2P_2(OR) + 2\ EtOH \rightarrow IrH_5P_2 + 2\ IrH_2P_2(CO)(CH_3) + 3\ ROH \qquad (31)$$

Reactions of acetaldehyde with $IrH_2P_2(OR)$. To examine the unusual coupling reaction of eq. 30, acetaldehyde, (MeCHO; 0.45 *M*) was added in increments of 0.15 *M* to a solution of $IrH_2P_2(OR)$ (1.0×10^{-2} *M*). Catalytic dimerization of the acetaldehyde resulted, to give 17 moles of $MeCO_2Et$ per mol $IrH_2P_2(OR)$ (eq. 32).

$$2\ CH_3CHO \xrightarrow{IrH_2P_2(OR)} CH_3CO_2CH_2CH_3 \qquad (32)$$

For the first two increments reaction was complete (room temperature) in less than 10 min, reflecting the remarkably high catalytic activity of $IrH_2P_2(OR)$ for the Tischenko reaction. After addition of the third increment unreacted MeCHO was observed and no $IrH_2P_2(OR)$ remained. The following iridium-containing products were identified: $IrH_2P_2(Me)(CO)$ (3.8×10^{-3} *M*), $IrH_3P_2(CO)$ (1.1×10^{-3} *M*), IrH_5P_2 (0.4×10^{-3} *M*), and $IrH_2P_2(\eta^2\text{-}O_2CMe)$ [13*] (0.5×10^{-3} *M*).

In an effort to gain some mechanistic insight into reaction 31, MeCHO was allowed to react with $IrH_2P_2(OR)$ and methanol (selected because it reacts more slowly with $IrH_2P_2(OR)$ than does ethanol). 0.11 ml of a solution of MeOH (1.2 M) and MeCHO (0.15 M) was added to 0.55 ml of a solution of $IrH_2P_2(OR)$ (15×10^{-3} M). The orange color changed rapidly to pale yellow. No formation of $MeCO_2Et$ was observed. Instead, all the MeCHO was consumed to form $MeCO_2Me$ (25×10^{-3} M) (eq. 33). The major metal containing product was IrH_5P_2 (11.6×10^{-3} M), along with minor amounts of $IrH_2P_2(Me)(CO)$ (1.2×10^{-3} M) and $IrH_3P_2(CO)$ (0.8×10^{-3} M).

$$2\ CH_3OH + 2\ CH_3CHO + IrH_2P_2(OR) \rightarrow 2\ CH_3CO_2CH_3 + IrH_5P_2 + ROH \tag{33}$$

This suggests that in the mechanism of acetaldehyde dimerization (eq. 32), the coupling of the two aldehyde molecules is preceded by the reduction of one molecule to an ethoxy group (either as free ethanol or as coordinated ethoxide). Thus, in the presence of an excess of MeOH, the alkoxy group which is present in large excess (methoxy) is incorporated in to the ester.

Attempted hydrogenation of unactivated esters. From the observations above with alcohols and aldehydes it would appear that the stoichiometric reduction of unactivated esters by IrH_5P_2, in contrast to that of CF_3COOR, is thermodynamically unfavorable (eq. 36). Thus, eq. 36 is the sum of two thermodynamically unfavorable reactions: (1) Reaction 34 is the reverse of reaction 30 which proceeds spontaneously. (2) Reaction 35, i.e. substitution of ROH by EtOH, also appears to be thermodynamically unfavorable as evidenced by the absence of substitution of OR by OMe in solutions containing $IrH_2P_2(OR)$ and MeOH.

$$IrH_5P_2 + MeCO_2Et + ROH \rightarrow IrH_2P_2(OR) + 2\ EtOH \quad \Delta G > 0 \tag{34}$$

$$IrH_2P_2(OR) + EtOH \rightarrow IrH_2P_2(OEt) + ROH \quad \Delta G > 0 \tag{35}$$

$$IrH_5P_2 + MeCO_2Et \rightarrow IrH_2P_2(OEt) + EtOH \quad \Delta G > 0 \tag{36}$$

Consistent with this, no reaction between methyl acetate (0.1 M) and IrH_5P_2 was observed under H_2 (13.5 h at 105°C) or in the absence of H_2 (12 h at 70°C). A solution of IrH_5P_2 (ca. 15×10^{-3} M), $MeCO_2CH_3$ (0.1 M), and $IrH_2P_2(OR)$ (ca. 15×10^{-3} M) exhibited no reaction after 48 h at 60°C.

Concluding remarks

The results reported in this paper provide further examples of the rich catalytic chemistry of transition metal polyhydride complexes. Distinctive features of these systems include the ability of such polyhydride complexes to serve as highly loaded "hydrogen reservoirs" and the accessibility of vacant coordination sites through the facile reductive elimination of coordinated hydrogen. These properties make such complexes particularly effective as catalysts for the hydrogenation of substrates such as arenes and esters that require more than two hydrogen atoms, [2,3] as well as for transferhydrogenation reactions. Figure 7 depicts a plausible mechanistic scheme for such transfer hydrogenation reactions [9*,10,12*]. The extremely high rates of transfer-hydrogenation observed for reaction 26 (complete hydrogenation of

$CH_2{=}CHCMe_3$ in 5 min at 30 °C when acetone is present initially) are, to our knowledge, unprecedented.

Experimental

All reactions were conducted under rigorously anaerobic conditions. IrH_5P_2 was prepared by the method of Clerici et al. [14]. $Ir(PPh_3)_2(CO)I$ was prepared by the reaction of $Ir(PPh_3)_2(CO)Cl$ (Aldrich) with excess NaI. Unless noted otherwise, all reactions were monitored by ^1H NMR spectroscopy and conducted in cyclohexane-d_{12}. Alkanes, toluene, benzene, tetramethyltetrahydrofuran, and THF were distilled from Na/K alloy before use. CF_3COOR was distilled from LiH. Acetaldehyde and acetone were distilled from $CaSO_4$. Isopropanol was distilled from $CaSO_4$ and then from Na and isopropylbenzoate.

^1H NMR spectra were determined with the University of Chicago Chemistry Department 500 MHz and Bruker 270 MHz spectrometers. Pulse angles of $< 20°$ and delay times of > 3 sec were used to ensure reliable integration values (confirmed in some cases by varying the delay time). Chemical shift values were calibrated using the $C_6D_{11}H$ resonance (δ 1.380) and concentrations were determined by reference to the integrated signal of a known concentration of hexamethylsiloxane (HMSO, δ 0.05). ^{19}F, ^{31}P, and ^{15}N NMR spectra were determined with a Nicolet 200 MHz spectrometer. FT-infrared spectra were recorded with a Nicolet 20 SXB spectrophotometer. ^{19}F and ^{31}P NMR were calibrated by recording samples of CCl_3F (δ 0.0) and trimethylphosphate (δ 0.0), respectively, in C_6D_{12} before and after the spectrum of interest was taken. No significant "drift" was observed between spectra.

Kinetic measurements, unless noted otherwise, were made by preparing a solution in an NMR tube in an inert atmosphere box, and sealing without evacuating the sample (under N_2). This greatly diminished the rate at which H_2, CF_3COOR, and other volatiles evaporated from the solution phase into the gas space during the course of the reaction. The Nicolet program KINET was used to obtain spectra at pre-set intervals. Temperatures were calibrated with either an ethylene glycol standard or an electronic thermocouple (calibrated against each other) but temperature fluctuations of up to ca. ± 0.8 °C may have ocurred during the course of a run. Rate constants were determined, unless noted otherwise, by monitoring the disappearance of IrH_5P_2 (up to at least 80% completion) by following the integral of the hydride resonance at δ -11.2. When possible (no overlap with product peaks) the result was confirmed by also monitoring the disappearance of the PCH resonance (δ 1.76) as well as any isolated product peaks. Hexamethyldisiloxane was used as an internal standard; when significant ($\pm 2\%$) deviations were found during the course of a run other integrals were adjusted accordingly. Unless noted otherwise, experiments that were part of a single series were performed on the same day so as to minimize error due to fluctuations in spectrometer temperature and other potential artifacts.

Preparation of $IrH_2P_2(OR)$. IrH_5P_2 (0.104 g, 0.2 mmol) was dissolved in hexanes (4.0 ml) and trifluoroethanol (0.044 ml, 0.6 mmol), followed by 3,3-dimethylbutene (0.104 ml, 0.8 mmol) with rapid stirring. Solvent and volatiles were then evaporated and the resulting orange solid was dried under high vacuum ($< 10^{-4}$ torr) for > 4 h. (Elemental analysis (Microanalytische Labs, W. Germany). Found: C, 39.00; H, 7.42; F, 9.37; P, 9.85. $C_{20}H_{46}F_3OIrP_2$ calcd.: C, 39.14; H, 7.55; F, 9.29; P, 10.09%. (See text and Table 1 for NMR spectral data). The material was then redissolved in 2 ml pentane to give a 0.1 M stock solution. $IRH_2P_2(OR)$ samples were obtained by evaporating appropriate aliquots as needed, thereby achieving accurate anaerobic measurements.

Molality determinations were made using the Signer apparatus, with pentane as solvent, and azobenzene (recrystallized from ethanol) as standard. $IrH_2P_2(OR)$ was prepared from a carefully weighed quantity of IrH_5P_2 by the above procedure, and then dissolved in a pentane solution which was used in its entirety for the measurement. Similar solutions were shown, by comparison with an internal standard, to contain one mol $IrH_2P_2(OR)$ per mol IrH_5P_2 used in preparation.

Dinitrogen complexes. The complexes $(IrH_3P_2)_n(N_2)$ ($n = 1, 2$) were prepared most effectively as follows. An O-ring valve NMR tube (William A. Sales Co.) containing a toluene-d_8 solution of $IrH_2P_2(OR)$ saturated with N_2 was attached to a high-vacuum line and evacuated at −78 °C, and then filled with a 90/10 mixture of N_2/H_2. To effect the passage of H_2 into solution from the above atmosphere, the tube was removed from the dry ice/acetone, briefly agitated, and then immediately reimmersed in the cold bath. This was repeated ca. 10 times after which the solution was allowed to stand in a cyclohexanone/dry ice bath (−45 °C) for ca. 10 min so that any H_2 in solution which may not have reacted could react at the higher temperature. This process was repeated. The NMR tube was then evacuated, N_2/H_2 was readmitted (in case the gas above the solution had been depleted of H_2) and the entire cycle repeated again. Finally the tube was evacuated and pure N_2 was introduced. In a typical experiment the resulting product distribution (As determined by ^1H NMR) was $IrH_3P_2(N_2)$ (1.40×10^{-3} M), $(IrH_2P_2)_2(N_2)$ (0.39×10^{-3} M), $IrH_2P_2(OR)$ (2.0×10^{-3} M), IrH_5P_2 (1.40×10^{-3} M). This sample was then evacuated, and at −35 °C the concentration of $IrH_3P_2(N_2)$ was found to decrease slowly while $[(IrH_3P_2)_2(N_2)]$ slightly increased; after ca. 170 min, concentrations of $IrH_3P_2(N_2)$ and $[(IrH_3P_2)_2(N_2)]$ were 0.66×10^{-3} M and 0.49×10^{-3} M, respectively. Dinitrogen (850 torr) was then reintroduced to the NMR tube and NMR revealed a significant increase in the concentration of $IrH_3P_2(N_2)$ at the expense of $[(IrH_3P_2)_2(N_2)]$. Upon remaining in the NMR probe at −35 °C the solution appeared to reach equilibrium (eq. 37) with the following concentrations: $IrH_3P_2(N_2)$, (1.14×10^{-3} M); $[(IrH_3P_2)_2(N_2)]$, (0.13×10^{-3} M).

$$(IrH_3P_2)_2(N_2) + N_2 \rightarrow 2\ IrH_3P_2(N_2) \qquad (37)$$

Assuming $[N_2] = (850/760) \times 5.9 \times 10^{-3}$ M [15*], we find that $K_{eq} \sim 1.5$. This should be regarded as a minimum value however due to the possibility that the N_2 in solution is not at equilibrium with atmospheric N_2. The product distribution resulting from the above preparation (i.e., ca. 50% unreacted $IrH_2P_2(OR)$ and ca. 5% IrH_5P_2; see above) suggests that the yield of the N_2 complexes could be improved either by increasing the number of cycles, or by using a gas mixture with a higher H_2 content.

Acknowledgements

We are grateful to the National Science Foundation for a grant in support of this research, to IBM Corporation for a Postdoctoral Fellowship (to A.S.G.) and to

Johnson–Matthey, Inc. for a generous loan of iridium. The NMR facilities used in this research were supported in part through the University of Chicago Cancer Center Grant No. NIH-CA-14559.

References

1 For a recent review see: G.G. Hlatky and R.H. Crabtree, Coord. Chem. Rev., 65 (1985) 1.

2 (a) G.P. Pez, R.A. Gray and J. Corsi, J. Am. Chem. Soc., 103 (1981) 7528; (b) R.A. Grey, G.P. Pez and A. Walls, ibid., 102 (1980) 5548; (c) R.A. Grey, F.P. Pez and A. Walls, ibid., 103 (1981 7536; (d) R.A. Grey, G.P. Pez, A. Walls and J. Corsi, J. Chem. Soc., Chem. Commun. (1980) 783.

3 (a) R. Wilczynski, W.A. Fordyce and J. Halpern, J. Am. Chem. Soc., 105 (1983) 2066; (b) W.A. Fordyce, R. Wilczynski and J. Halpern, J. Organomet. Chem., 296 (1985) 115; (c) D.E. Linn, Jr. and J. Halpern, J. Am. Chem. Soc., 109 (1987) 2969; (d) D.E. Linn, Jr. and J. Halpern, J. Organomet. Chem., 330 (1987) 155.

4 A.S. Goldman and J. Halpern, J. Am. Chem. Soc., 109 (1987) 7537.

5 Deuterated aromatic solvents could not be used in these studies because of facile isotopic exchange with $[IrH_5P_2]$.

6 B.R. James, M. Preece, and S.D. Robinson, Adv. Chem. Ser., 196 (1982) 145.

7 D.H. Empsall, E.M. Hyde, E. Mentzer, B.L. Shaw and M.F. Uttley, J. Chem. Soc., Dalton, (1976) 2069.

8 B.E. Mann, C. Masters and B.L. Shaw, J. Inorg. Nucl. Chem., 33 (1971) 2204; (b) J. Chatt, R.S. Coffey and B.L. Shaw, J. Chem. Soc., (1965) 7391.

9 IrH_5P_2-catalyzed transfer hydrogenation by alcohols, albeit at much higher temperatures, has recently been reported independently by Lin et al. (a) Y. Lin, D. Ma and X. Lu, J. Organomet. Chem., 323 (1987) 407; (b) Y. Lin, D. Ma and X. Lu, Tetrahedron Lett., 28 (1987) 3115.

10 (a) H. Felkin, T. Fillebeen-Kahn, Y. Gault, R. Holmes-Smith, J. Zakrzewski, Tetrahedron Lett., 25 (1984) 1279; (b) H. Felkin, T. Fillebeen-Kahn, R. Holmes-Smith, Y. Yingrui, ibid., 26 (1985) 1999.

11 E.F. Still, D.R. Westrum and G.C. Sinke, The Chemical Thermodynamics of Organic Compounds, J. Wiley, New York, 1969.

12 The concentration of $CH_3CH_2CMe_3$ exceeded that attributable to reduction by IrH_5P_2 by ca. 3×10^{-3} *M*. This is attributed to transfer-hydrogenation (deuterogenation) by the C_6D_{12} solvent.

13 $IrH_2P_2(\eta^2\text{-}O_2CCH_3)$ was identified in part by its ^1H NMR hydride resonance, δ −31.7, t, $^2J(HP)$ 15.2 Hz, in comparison with that of $IrH_2P_2(\eta^2\text{-}O_2CCF_3)$ (δ −33.3, t, $^2J(HP)$ 14.7 Hz).

14 M.G. Clerici, S. DiGioacchino, F. Maspero, E. Perrotti and A. Zanobi, J. Organomet. Chem., 84 (1975) 3115.

15 Adapted from Landolt-Bornstein, Zahlenwerte und Funktionen, 6th Ed., Vol. 2, Part 2b, Springer-Verlag, Berlin, 1962.